EPJ Web of Conferences **168**, 01006 (2018) https://doi.org/10.1051/epjconf/201816801006
Joint International Conference of ICGAC-XIII and IK-15 on Gravitation, Astrophysics and Cosmology

The binary progenitors of short and long GRBs and their gravitational-wave emission

J. A. Rueda[1,2,3,⋆], *R.* Ruffini[1,2,3,4], *J. F.* Rodriguez[1,2], *M.* Muccino[1,2], *Y.* Aimuratov[1,2], *U.* Barres de Almeida[3], *L.* Becerra[1,2], *C. L.* Bianco[1,2], *C.* Cherubini[5,6], *S.* Filippi[5,6], *M.* Kovacevic[1,2], *R.* Moradi[1,2], *G. B.* Pisani[1,2], and *Y.* Wang[1,2]

[1] *Dipartimento di Fisica and ICRA, Sapienza Università di Roma, P.le Aldo Moro 5, I–00185 Rome, Italy*
[2] *ICRANet, P.zza della Repubblica 10, I–65122 Pescara, Italy*
[3] *ICRANet-Rio, Centro Brasileiro de Pesquisas Físicas, Rua Dr. Xavier Sigaud 150, 22290–180 Rio de Janeiro, Brazil*
[4] *Université de Nice Sophia Antipolis, CEDEX 2, Grand Château Parc Valrose, Nice,*
[5] *Unit of Nonlinear Physics and Mathematical Modeling, Università Campus Bio-Medico di Roma, Via A. del Portillo 21, I–00128 Rome, Italy*
[6] *ICRA, Università Campus Bio-Medico di Roma, Via A. del Portillo 21, I–00128 Rome, Italy*

Abstract. We have sub-classified short and long-duration gamma-ray bursts (GRBs) into seven families according to the binary nature of their progenitors. Short GRBs are produced in mergers of neutron-star binaries (NS-NS) or neutron star-black hole binaries (NS-BH). Long GRBs are produced via the induced gravitational collapse (IGC) scenario occurring in a tight binary system composed of a carbon-oxygen core (CO_{core}) and a NS companion. The CO_{core} explodes as type Ic supernova (SN) leading to a hypercritical accretion process onto the NS: if the accretion is sufficiently high the NS reaches the critical mass and collapses forming a BH, otherwise a massive NS is formed. Therefore long GRBs can lead either to NS-BH or to NS-NS binaries depending on the entity of the accretion. We discuss for the above compact-object binaries: 1) the role of the NS structure and the nuclear equation of state; 2) the occurrence rates obtained from X and gamma-rays observations; 3) the predicted annual number of detections by the Advanced LIGO interferometer of their gravitational-wave emission.

1 Introduction

There has been a traditional phenomenological classification of gamma-ray bursts (GRBs) based on the observed prompt duration, T_{90}: long GRBs for $T_{90} > 2$ s and short GRBs for $T_{90} < 2$ s[1–5]. Progress has been made in the meantime in the understanding of the nature of both long and short GRBs leading to a physical, instead of empirical, classification of GRBs based on the progenitor systems [6–8].

⋆e-mail: jorge.rueda@icra.it

1.1 Long GRBs

In the case of long GRBs we stand on the induced gravitational collapse (IGC) scenario that introduces as their progenitors short-period binaries composed of a carbon-oxygen core (CO_{core}) with a NS companion [9–15]. The core-collapse of the CO_{core}, which forms a NS as central remnant (hereafter νNS), leads also to a SN explosion that triggers a massive, hypercritical accretion process onto the NS companion. The parameters of the *in-state*, i.e. of the CO_{core}-NS binary, lead to two sub-classes of long GRBs with corresponding *out-states* [6]:

- *X-ray flashes (XRFs)*. Long bursts with $E_{iso} \lesssim 10^{52}$ erg are produced by CO_{core}-NS binaries with relatively large binary separations ($a \gtrsim 10^{11}$ cm). The accretion rate of the SN ejecta onto the NS in these systems is not high enough to bring the NS mass to the critical value M_{crit}, hence no BH is formed. The out-state of this GRB sub-class can be either a νNS-NS binary if the system keeps bound after the SN explosion, or two runaway NSs if the binary system is disrupted.
- *Binary driven hypernovae (BdHNe)*. Long bursts with $E_{iso} \gtrsim 10^{52}$ erg are instead produced by more compact CO_{core}-NS binaries ($a \lesssim 10^{11}$ cm, see e.g., Refs. [13, 15]). In this case the SN triggers a larger accretion rate onto the NS companion, e.g. $\gtrsim 10^{-2}$–10^{-1} $M_\odot$ s^{-1}, bringing the NS to its critical mass M_{crit},[11–13] namely to the point of gravitational collapse with consequent formation of a BH. Remarkably, in Ref. [14] it was recently shown that the large majority of BdHNe leads naturally to NS-BH binaries owing to the high compactness of the binary that avoids the disruption of it even in cases of very high mass loss exceeding 50% of the total mass of the initial CO_{core}-NS binary.

In addition, it exists the possibility of *BH-SNe*.[6] Long burst with $E_{iso} \gtrsim 10^{54}$ erg occurring in close CO_{core}-BH binaries in which the hypercritical accretion produces, as *out-states*, a more massive BH and a νNS. These systems have been considered in Ref. [6] as a subset of the BdHNe but no specific example have been yet observationally identified.

1.2 Short GRBs

There is the consensus within the GRB community that the progenitors of short GRBs are mergers of NS-NS and/or NS-BH binaries (see, e.g., Refs. [16–19], and Ref. [20], for a recent review). Similarly to the case of long GRBs, in Ref. [6] short GRBs have been split into different sub-classes:

- *Short gamma-ray flashes (S-GRFs)*. Short bursts with energies $E_{iso} \lesssim 10^{52}$ erg, produced when the post-merger core do not surpass the NS critical mass M_{crit}, hence there is no BH formation. Thus these systems left as byproduct a massive NS and possibly, due to the energy and angular momentum conservation, orbiting material in a disk-like structure or a low-mass binary companion.
- *Authentic short gamma-ray bursts (S-GRBs)*. Short bursts with $E_{iso} \gtrsim 10^{52}$ erg, produced when the post-merger core reaches or overcome M_{crit}, hence forming a Kerr or Kerr-Newman BH,[8] and also in this case possibly orbiting material.
- *Ultra-short GRBs (U-GRBs)*. A new sub-class of short bursts originating from νNS-BH merging binaries. They can originate from BdHNe (see Ref. [14]) or from BH-SNe.

In addition, it exists the possibility of *gamma-ray flashes (GRFs)*. These are bursts with hybrid properties between short and long, they have $10^{51} \lesssim E_{iso} \lesssim 10^{52}$ erg. This sub-class of sources originates in NS-WD mergers.[6]

We focus here on the physical properties of the above progenitors, as well as on the main properties of NSs that play a relevant role in the dynamics of these systems and that lead to the above different GRB sub-classes. We shall discuss as well recent estimates of the rates of occurrence on all the above

subclasses based on X and gamma-ray observations, and also elaborate on the possibility of detecting the gravitational wave (GW) emission originated in these systems.

2 IGC, Hypercritical Accretion, and Long GRBs

We turn now to the details of the accretion process within the IGC scenario. Realistic simulations of the IGC process were performed in Ref. [12], including: 1) detailed SN explosions of the CO_{core}; 2) the hydrodynamic details of the hypercritical accretion process; 3) the evolution of the SN ejecta material entering the Bondi-Hoyle region all the way up to its incorporation into the NS. Here the concept of hypercritical accretion refers to the fact the accretion rates are highly super-Eddington. The accretion process in the IGC scenario is allowed to exceed the Eddington limit mainly for two reasons: i) the photons are trapped within the infalling material impeding them to transfer momentum; ii) the accreting material creates a very hot NS atmosphere ($T \sim 10^{10}$ K) that triggers a very efficient neutrino emission which become the main energy sink of these systems unlike photons.

The hypercritical accretion process in the above simulations was computed within a spherically symmetric approximation. A further step was given in Ref. [13] by estimating the angular momentum that the SN ejecta carries and transfer to the NS via accretion, and how it affects the evolution and fate of the system. The calculations are as follows: first the accretion rate onto the NS is computed adopting an homologous expansion of the SN ejecta and introducing the pre-SN density profile of the CO_{core} envelope from numerical simulations. Then, it is estimated the angular momentum that the SN material might transfer to the NS: it comes out that the ejecta have enough angular momentum to circularize for a short time and form a disc around the NS. Finally, the evolution of the NS central density and rotation angular velocity (spin-up) is followed computing the equilibrium configurations from the numerical solution of the axisymmetric Einstein equations in full rotation, until the critical point of collapse of the NS to a BH taking into due account the equilibrium limits given by mass-shedding and the secular axisymmetric instability.

Now we enter into the details of each of the above steps. The accretion rate of the SN ejecta onto the NS can be estimated via the Bondi-Hoyle-Lyttleton accretion formula:

$$\dot{M}_B(t) = \pi\rho_{\rm ej}R_{\rm cap}^2\sqrt{v_{\rm rel}^2+c_{\rm s,ej}^2}, \qquad R_{\rm cap}(t) = \frac{2GM_{\rm NS}(t)}{v_{\rm rel}^2+c_{\rm s,ej}^2}, \tag{1}$$

where G is the gravitational constant, $\rho_{\rm ej}$ and $c_{\rm s,ej}$ are the density and sound speed of the SN ejecta, $R_{\rm cap}$ is the NS gravitational capture radius (Bondi-Hoyle radius), $M_{\rm NS}$, the NS mass, and $v_{\rm rel}$ the ejecta velocity relative to the NS: $\vec{v}_{\rm rel} = \vec{v}_{\rm orb} - \vec{v}_{\rm ej}$, with $|\vec{v}_{\rm orb}| = \sqrt{G(M_{\rm core}+M_{\rm NS})/a}$, the module of the NS orbital velocity around the CO_{core}, and $\vec{v}_{\rm ej}$ the velocity of the supernova ejecta (see Fig. 1).

Extrapolating the results for the accretion process from stellar wind accretion in binary systems, the angular momentum per unit time that crosses the NS capture region can be approximated by:$\dot{L}_{\rm cap} = (\pi/2)\left(\epsilon_\rho/2 - 3\epsilon_v\right)\rho_{\rm ej}(a,t)v_{\rm rel}^2(a,t)R_{\rm cap}^4(a,t)$, where ϵ_ρ and ϵ_v are parameters measuring the inhomogeneity of the flow (see Ref. [13] for details).

In order to simulate the hypercritical accretion it is adopted an homologous expansion of the SN ejecta, i.e. the ejecta velocity evolves as $v_{\rm ej}(r,t) = nr/t$, where r is the position of every ejecta layer from the SN center and n is called expansion parameter. The ejecta density is given by $\rho_{\rm ej}(r,t) = \rho_{\rm ej}^0(r/R_{\rm star}(t),t_0)\frac{M_{\rm env}(t)}{M_{\rm env}(0)}\left(\frac{R_{\rm star}(0)}{R_{\rm star}(t)}\right)^3$, where $M_{\rm env}(t)$ the mass of the CO_{core} envelope, namely the mass of the ejected material in the SN explosion and available to be accreted by the NS, $R_{\rm star}(t)$ is the position of the outermost layer of the ejected material, and $\rho_{\rm ej}^0$ is the pre-SN density profile. The latter can be approximated with a power law: $\rho_{\rm ej}(r,t_0) = \rho_{\rm core}(R_{\rm core}/r)^m$, where $\rho_{\rm core}$, $R_{\rm core}$ and m are the profile parameters which are fixed by fitting the pre-SN profiles obtained from numerical simulations.

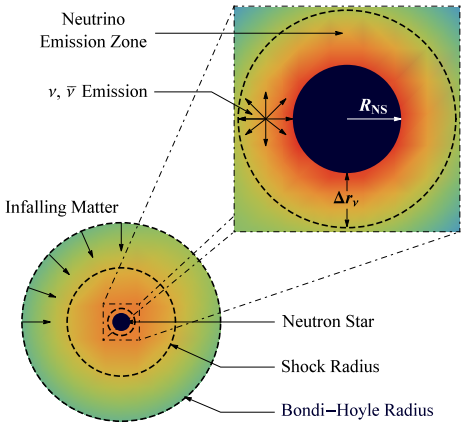

Figure 1. Scheme of the IGC scenario: the CO_{core} undergoes SN explosion, the NS accretes part of the SN ejecta and then reaches the critical mass for gravitational collapse to a BH, with consequent emission of a GRB. The SN ejecta reach the NS Bondi-Hoyle radius and fall toward the NS surface. The material shocks and decelerates as it piles over the NS surface. At the neutrino emission zone, neutrinos take away most of the infalling matter gravitational energy gain. The neutrinos are emitted above the NS surface in a region of thickness Δr_ν about half the NS radius that allow the material to reduce its entropy to be finally incorporated to the NS. The image is not to scale. For further details and numerical simulations of the above process see Refs. [12, 13, 15].

For the typical parameters of pre-SN CO_{core} and assuming a velocity of the outermost SN layer $v_{\rm sn}(R_{\rm star}, t_0) \sim 10^9$ cm s^{-1} and a free expansion $n = 1$ (for details of typical initial conditions of the binary system see Refs. [12] and [13]), Eq. (1) gives accretion rates around the order of $10^{-4} - 10^{-2} M_\odot$ s^{-1}, and an angular momentum per unit time crossing the capture region $\dot{L}_{\rm cap} \sim 10^{46}$–$10^{49}$ g cm^2 s^{-2}.

We consider the NS companion of the CO_{core} initially as non-rotating, thus at the beginning the NS exterior spacetime is described by the Schwarzschild metric. The SN ejecta approach the NS with specific angular momentum, $l_{\rm acc} = \dot{L}_{\rm cap}/\dot{M}_B$, thus they will circularize at a radius $r_{\rm st}$ if they have enough angular momentum. What does the word "enough" means here? The last stable circular orbit (LSO) around a non-rotating NS is located at a distance $r_{\rm lso} = 6GM_{\rm NS}/c^2$ and has an angular momentum per unit mass $l_{\rm lso} = 2\sqrt{3}GM_{\rm NS}/c$. The radius $r_{\rm lso}$ is larger than the NS radius for masses larger than 1.67 $M_\odot$, 1.71 $M_\odot$, and 1.78 $M_\odot$ for the GM1, TM1, and NL3 nuclear equation of state (EOS).[13] If $l_{\rm acc} \geq l_{\rm lso}$ the material circularizes around the NS at locations $r_{\rm st} \geq r_{\rm lso}$. For the values of the IGC systems under discussion here, $r_{\rm st}/r_{\rm lso} \sim 10 - 10^3$, thus the SN ejecta have enough angular momentum to form a sort of disc around the NS. Even in this case, the viscous forces and other angular momentum losses that act on the disk will allow the matter in the disk to reach the inner boundary at $r_{\rm in} \sim r_{\rm lso}$, to then be accreted by the NS.

Within this picture, the NS accretes the material from $r_{\rm in}$ and the NS mass and angular angular momentum evolve as:

$$\dot{M}_{\rm NS} = \left(\frac{\partial M_{\rm NS}}{\partial M_b}\right)_{J_{\rm NS}} \dot{M}_b + \left(\frac{\partial M_{\rm NS}}{\partial J_{\rm NS}}\right)_{M_b} \dot{J}_{\rm NS}, \qquad \dot{J}_{\rm NS} = \xi\, l(r_{\rm in}) \dot{M}_{\rm B}, \tag{2}$$

where M_b is the NS baryonic mass, $l(r_{\rm in})$ is the specific angular momentum of the accreted material at $r_{\rm in}$, which corresponds to the angular momentum of the LSO, and $\xi \leq 1$ is a parameter that measures the efficiency of angular momentum transfer. We assume in our simulations $\dot{M}_b = \dot{M}_B$. The baryonic and gravitational mass are related by [21]:

$$\frac{M_b}{M_\odot} = \frac{M_{\rm NS}}{M_\odot} + \frac{13}{200}\left(\frac{M_{\rm NS}}{M_\odot}\right)^2 \left(1 - \frac{1}{137} j_{\rm NS}^{1.7}\right), \tag{3}$$

where $j_{\rm NS} \equiv cJ_{\rm NS}/(GM_\odot^2)$. In addition, since the NS will spin up with accretion, we need information of the dependence of the specific angular momentum of the LSO as a function of both the NS mass

Table 1. Critical NS mass in the non-rotating case and constants k and p needed to compute the NS critical mass in the non-rotating case given by Eq. (5). The values are given for the NL3, GM1 and TM1 EOS.

EOS	$M_{\rm crit}^{J=0}\,(M_\odot)$	p	k
NL3	2.81	1.68	0.006
GM1	2.39	1.69	0.011
TM1	2.20	1.61	0.017

and angular momentum. For corotating orbits the following relation is valid for all the aforementioned EOS:[13]

$$l_{\rm lso} = \frac{GM_{\rm NS}}{c}\left[2\sqrt{3} - 0.37\left(\frac{j_{\rm NS}}{M_{\rm NS}/M_\odot}\right)^{0.85}\right]. \tag{4}$$

The NS accretes mass until it reaches a region of instability. There are two main instability limits for rotating NSs: mass-shedding or Keplerian limit and the secular axisymmetric instability. The critical NS mass along the secular instability line is approximately given by:[21]

$$M_{\rm NS}^{\rm crit} = M_{\rm NS}^{J=0}(1 + k j_{\rm NS}^{p}), \tag{5}$$

where the parameters k and p depends of the nuclear EOS (see Table 1). These formulas fit the numerical results with a maximum error of 0.45%.

2.1 Most recent simulations of the IGC process

Additional details and improvements of the hypercritical accretion process leading to XRFs and BdHNe have been recently presented in Ref. [15]. In particular:

1. It was there improved the accretion rate estimate including the density profile finite size/thickness and additional $\rm CO_{core}$ progenitors leading to different SN ejecta masses were also considered.

2. It was shown in Ref. [13] the existence of a maximum orbital period, $P_{\rm max}$, over which the accretion onto NS companion is not high enough to bring it to the critical mass for gravitational collapse to a BH. Therefore, $\rm CO_{core}$-NS binaries with $P > P_{\rm max}$ lead to XRFs while the ones with $P \lesssim P_{\rm max}$ lead to BdHNe. In Ref. [15] the determination of $P_{\rm max}$ was extended to all the possible initial values of the mass of the NS companion and the angular momentum transfer efficiency parameter was also allowed to vary.

3. It was computed the expected luminosity during the hypercritical accretion process for a wide range of binary periods covering XRFs and BdHNe.

4. It was there shown that the presence of the NS companion originates large asymmetries (see, e.g., simulation in Fig. 2) in the SN ejecta leading to observable signatures in the X-rays.

Fig. 2 shows a simulation of an IGC process presented in Ref. [15]. We considered the effects of the gravitational field of the NS on the SN ejecta including the orbital motion as well as the changes in the NS gravitational mass owing to the accretion process via the Bondi formalism. The supernova matter was described as formed by point-like particles whose trajectory was computed by solving the Newtonian equation of motion. The initial conditions of the SN ejecta are computed assuming an homologous velocity distribution in free expansion. The initial power-law density profile of the CO

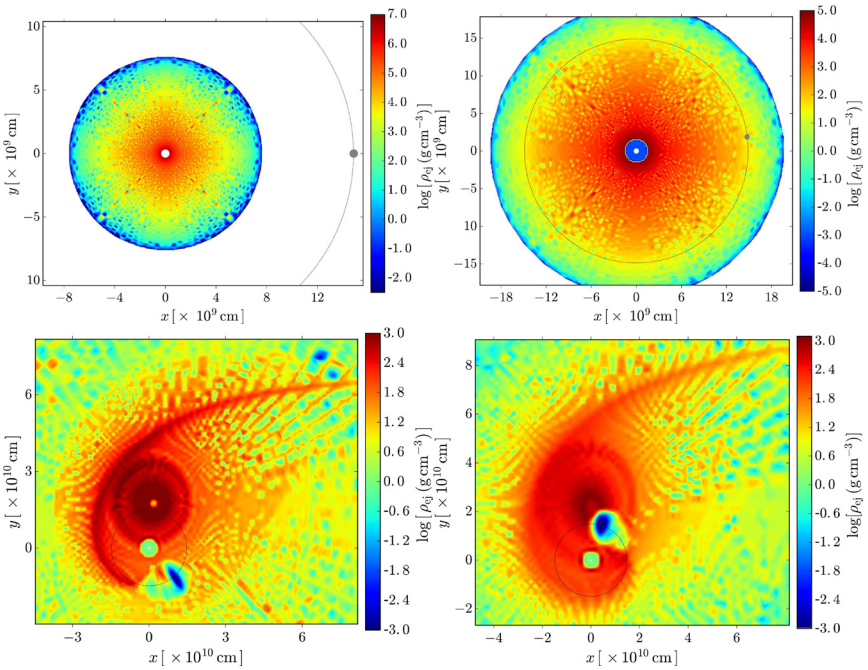

Figure 2. Hypercritical accretion process in the IGC binary system at selected evolution times. In this example the CO_{core} has a total mass of 9.44 $M_\odot$ divided in an ejecta mass of 7.94 $M_\odot$ and a νNS of 1.5 $M_\odot$ formed by the collapsed high density core. The supernova ejecta evolve homologously with outermost layer velocity $v_{0,\mathrm{star}} = 2\times10^9$ cm s^{-1}. The NS binary companion has an initial mass of 2.0 $M_\odot$. The binary period is $P \approx 5$ min, which corresponds to a binary separation $a \approx 1.5\times10^{10}$ cm. The system of coordinates is centered on the νNS represented by the white-filled circle at $(0,0)$. The NS binary companion, represented by the gray-filled circle, orbits counterclockwise following the thin-dashed circular trajectory. The colorbar indicates values of ejecta density in logarithmic scale. *Left upper panel:* initial time of the process. The supernova ejecta expand radially outward and the NS binary companion is at $(a,0)$. *Right upper panel:* the accretion process starts when the first supernova layers reach the Bondi-Hoyle region. This happens at $t = t_{\mathrm{acc},0} \approx a/v_{0,\mathrm{star}} \approx 7.7$ s. *Left lower panel:* the NS binary companion reaches the critical mass by accreting matter from the SN with consequent collapse to a BH. This happens at $t = t_{\mathrm{coll}} \approx 254$ s $\approx 0.85\,P$. The newly-formed BH of mass $M_{\mathrm{BH}} = M_{\mathrm{crit}} \approx 3\,M_\odot$ is represented by the black-filled circle. It is here evident the asymmetry of the supernova ejecta induced by the presence of the accreting NS companion at close distance. *Right lower panel:* $t = t_{\mathrm{coll}} + 100$ s $= 354$ s $\approx 1.2P$, namely 100 s after the BH formation. It appears here the new binary system composed of the νNS and the newly-formed BH.

envelope is simulated by populating the inner layers with more particles. For the $M_{\mathrm{ZAMS}} = 30\,M_\odot$ progenitor which gives a CO_{core} with envelope profile $\rho^0_{\mathrm{ej}} \approx 3.1\times10^8(8.3\times10^7/r)^{2.8}$ g cm^{-3}, we adopt for the simulation a total number of $N = 10^6$ particles. We assume that particles crossing the Bondi-Hoyle radius are captured and accreted by the NS so we removed them from the system as they reach that region. We removed these particles according to the results obtained from the numerical integration explained above. Fig. 2 shows the orbital plane of an IGC binary at selected times of its evolution. The NS has an initial mass of 2.0 $M_\odot$; the CO_{core} leads to a total ejecta mass 7.94 $M_\odot$ and a νNS of 1.5 $M_\odot$. The orbital period of the binary is $P \approx 5$ min, i.e. a binary separation $a \approx 1.5\times10^{10}$ cm. For these parameters the NS reaches the critical mass and collapses to form a BH.

2.2 Post-Explosion Orbits and Formation of NS-BH Binaries

We have seen how in BdHNe the accretion process can lead to BH formation in a time-interval as short as the orbital period. We here deepen this analysis to study the effect of the SN explosion in such a scenario following Ref. [14]. As the ejecta timescale becomes a fraction of the orbital one, the fate of the post-explosion binary is altered. For these models, we assumed tight binaries in circular orbit with an initial orbital separation of 7×10^9 cm. With CO_{core} radii of $1\text{–}4\times10^9$ cm, such a separation is small, but achievable. The binary consists of a CO_{core} and a 2.0 $M_\odot$ NS companion. When the CO_{core} collapses, it forms a 1.5 $M_\odot$ NS, ejecting the rest of the core. We then vary the ejecta mass and time required for most of the ejected matter to move out of the binary. Ref. [14] showed that even if 70% of the mass is lost from the system (in the 8 $M_\odot$ ejecta case), the system remains bound as long as the explosion time is just above the orbital time ($T_{\rm orbit} = 180$ s) with semi-major axes of less than 10^{11} cm.

The tight compact binaries produced in these explosions will emit GWs driving the system to merge. For typical massive star binaries, the merger time is many Myr. For BdHNe, the merger time is typically 10^4 yr, or less [14]. Since the merger should occur within the radius swept clean by the BdHN we expect a small baryonic contamination around the merger site which might lead to a new family of events which we term ultrashort GRBs, U-GRBs, to this new family of events.

3 NS-NS/NS-BH mergers and Short GRBs

Let us turn to short GRBs. We first proceed to estimate the mass and the angular momentum of the post-merger core via baryonic mass and angular momentum conservation of the system. We adopt for simplicity that non-rotating binary components. We first compute the total baryonic mass of the NS-NS binary $M_b = M_{b_1} + M_{b_2}$ using the relation between the gravitational mass M_i and the baryonic mass M_{b_i} ($i = 1, 2$) recently obtained in Ref. [21] and given in Eq. (3) assuming $j_{\rm NS} = cJ_{\rm NS}/(GM_\odot^2) = 0$. The post-merger core will have approximately the entire baryonic mass of the initial binary, i.e. $M_{b,\rm core} \approx M_b$, since little mass is expected to be ejected during the coalescence process. However, the gravitational mass of the post-merger core cannot be estimated using again the above formula since, even assuming non-rotating binary components, the post-merger core will necessarily acquire a fraction $\eta \leq 1$ of the binary angular momentum at the merger point. One expects a value of η smaller than unity since, during the coalesce, angular momentum is loss e.g. by gravitational wave emission and it can be also redistributed e.g. into a surrounding disk.

To obtain the gravitational mass of the post-merger core, we can use again Eq. (3) relating the baryonic mass $M_{b,\rm NS}$ and the gravitational mass $M_{\rm NS}$ in this case with $j_{\rm NS} \neq 0$. The mass and angular momentum of the post-merger core, respectively $M_{\rm core}$ and $J_{\rm core}$, are therefore obtained from baryon mass and angular momentum conservation, i.e.: $M_{\rm core} = M_{\rm NS}$, $M_{b,\rm core} = M_{b,\rm NS} = M_{b_1} + M_{b_2}$, $J_{\rm core} = J_{\rm NS} = \eta J_{\rm merger}$, where $J_{\rm merger}$ is the system angular momentum at the merger point. The value of $J_{\rm merger}$ is approximately given by $J_{\rm merger} = \mu r_{\rm merger}^2 \Omega_{\rm merger}$, where $\mu = M_1 M_2/M$ is the binary reduced mass, $M = M_1 + M_2$ is the total binary mass, and $r_{\rm merger}$ and $\Omega_{\rm merger}$ are the binary separation and angular velocity at the merger point. If we adopt the merger point where the two stars enter into contact we have $r_{\rm merger} = R_1 + R_2$, where R_i is the radius (which depend on the EOS) of the i-component of the binary.

Given the parameters of the merging binary, the above equations lead to the merged core properties. For the sake of exemplifying, let us assume a mass-symmetric binary, $M_1 = M_2 = M/2$. In this case the above equations lead to the angular momentum of the merged core $J_{\rm core} = (\eta/4)(GM^2/c)\mathcal{C}^{-1/2}$, where $\mathcal{C} \equiv GM_1/(c^2R_1) = GM_2/(c^2R_2)$ is the compactness of the merging binary components. Therefore, if we adopt $M_1 = 1.4$ $M_\odot$ and $\mathcal{C} = 0.15$, $M_{\rm core} = (2.61, 2.65)$ $M_\odot$ for

$\eta = (0, 1)$, i.e. for a dimensionless angular momentum of the merged core $j_{\rm core} = (0, 5.06)$. Whether or not these pairs ($M_{\rm core}$, $j_{\rm core}$) correspond to stable NSs depend on the nuclear EOS. A similar analysis can be done for any other pair of binary masses.

4 Detectability of GWs produced by the GRB progenitors

Having established the nature of the progenitors of each GRB sub-class, we turn now to briefly discuss the detectability of their associated GW emission. The minimum GW frequency detectable by the broadband aLIGO interferometer is $f_{\rm min}^{\rm aLIGO} \approx 10$ Hz.[35] Since during the binary inspiral the GW frequency is twice the orbital one, this implies that a binary enters the aLIGO band for orbital periods $P_{\rm orb} \lesssim 0.2$ s. Thus, $CO_{\rm core}$-NS binaries, *in-states* of XRFs and BdHNe, and $CO_{\rm core}$-BH binaries, *in-states* of BH-SN, are not detectable by aLIGO since they have orbital periods $P_{\rm orb} \gtrsim 5$ min $\gg 0.2$ s. Concerning their *out-states* after the corresponding hypercritical accretion processes, namely νNS-NS, *out-states* of XRFs, and νNS-BH, *out-states* of BdHNe and BH-SNe, they are not detectable by aLIGO at their birth but only when approaching the merger. Clearly, the analysis of the νNS-NS mergers is included in the analysis of the S-GRFs and S-GRBs and, likewise, the merger of νNS-BH binaries is included in the analysis of U-GRBs. In the case of NS-WD binaries the WD is tidally disrupted by the NS making their GW emission hard to be detected (see, e.g., Ref. [36]).

A coalescing binary evolves first through the *inspiral regime* to then pass over a *merger regime*, the latter composed by the plunge leading to the merger itself and by the ringdown (oscillations) of the newly formed object. During the inspiral regime the system evolves through quasi-circular orbits and is well described by the traditional point-like quadrupole approximation.[37–39] The GW frequency is twice the orbital frequency ($f_s = 2f_{\rm orb}$) and grows monotonically. The energy spectrum during the inspiral regime is: $dE/df_s = (1/3)(\pi G)^{2/3} M_c^{5/3} f_s^{-1/3}$, where $M_c = \mu^{3/5} M^{2/5} = \nu^{3/5} M$ is the so-called *chirp mass* and $\nu \equiv \mu/M$ is the symmetric mass-ratio parameter. A symmetric binary ($m_1 = m_2$) corresponds to $\nu = 1/4$ and the test-particle limit is $\nu \to 0$. The GW spectrum of the merger regime is characterized by a GW burst.[40] Thus, one can estimate the contribution of this regime to the signal-to-noise ratio with the knowledge of the location of the GW burst in the frequency domain and of the energy content. The frequency range spanned by the GW burst is $\Delta f = f_{\rm qnm} - f_{\rm merger}$, where $f_{\rm merger}$ is the frequency at which the merger starts and $f_{\rm qnm}$ is the frequency of the ringing modes of the newly formed object after the merger, and the energy emitted is $\Delta E_{\rm merger}$. With these quantities defined, one can estimate the typical value of the merger regime spectrum as: $dE/df_s \approx \Delta E_{\rm merger}/\Delta f$. Unfortunately, the frequencies and energy content of the merger regime of the above merging binaries are such that it is undetectable by LIGO.[41].

Since the GW signal is deep inside the detector noise, the signal-to-noise ratio (ρ) is usually estimated using the matched filter technique.[42] The exact position of the binary relative to the detector and the orientation of the binary rotation plane are usually unknown, thus it is a common practice to average over all the possible locations and orientations, i.e.:[42] $\langle \rho^2 \rangle = 4 \int_0^\infty \langle |\tilde{h}(f)|^2 \rangle / S_n(f) df = 4 \int_0^\infty h_c^2(f)/[f^2 S_n(f)] df$, where f is the GW frequency in the detector frame, $\tilde{h}(f)$ is the Fourier transform of $h(t)$, and $\sqrt{S_n(f)}$ is the one-sided amplitude spectral density of the detector noise, and $h_c(f)$ is the characteristic strain, $h_c = (1+z)/(\pi d_l) \sqrt{(1/10)(G/c^3)(dE/df_s)}$. We recall that in the detector frame the GW frequency is redshifted by a factor $1+z$ with respect to the one in the source frame, f_s, i.e. $f = f_s/(1+z)$ and d_l is the luminosity distance to the source. We adopt a ΛCDM cosmology with $H_0 = 71$ km s^{-1} Mpc^{-1}, $\Omega_M = 0.27$ and $\Omega_\Lambda = 0.73$.[43]

A threshold $\rho_0 = 8$ in a single detector is adopted by LIGO.[44] This minimum ρ_0 defines a maximum detection distance or GW horizon distance, say $d_{\rm GW}$, that corresponds to the most optimistic case when the binary is just above the detector and the binary plane is parallel to the detector plane.

In order to give an estimate the annual number of merging binaries associated with the above GRB sub-classes detectable by aLIGO we can use the lower and upper values of the aLIGO *search volume* defined by $\mathcal{V}_s = V_{\rm max}^{\rm GW}\mathcal{T}$, where $V_{\rm max}^{\rm GW} = (4\pi/3)\mathcal{R}^3$, where $\mathcal{T}$ is the observing time and $\mathcal{R}$ is the so-called *detector range* defined by $\mathcal{R} = \mathcal{F}\,d_{\rm GW}$, with $\mathcal{F}^{-1} = 2.2627$ (see, Ref. [44, 45], for details). For a (1.4+1.4) $M_\odot$ NS binary and the three following different observational campaigns we have:[44] 2015/2016 (O1; $\mathcal{T}$ = 3 months) $\mathcal{V}_S$ = (0.5–4) $\times 10^5$ Mpc^3 yr, 2017/2018 (O3; $\mathcal{T}$ = 9 months) $\mathcal{V}_S$ = (3–10)$\times 10^6$ Mpc^3 yr, and the entire network including LIGO-India at design sensitivity (2022+; $\mathcal{T}$ = 1 yr) $\mathcal{V}_S = 2 \times 10^7$ Mpc^3 yr. The maximum possible sensitivity reachable in 2022+ leads to $d_{\rm GW} \approx 0.2$ Gpc, hence $V_{\rm max}^{\rm GW} \approx 0.033$ Gpc^3, for such a binary. One can use this information for other binaries with different masses taking advantage of the fact that $d_{\rm GW}$ scales with the binary chirp mass as $M_c^{5/6}$. The expected GW detection rate by aLIGO can be thus estimated as: $\dot{N}_{\rm GW} \equiv \rho_{\rm GRB} V_{\rm max}^{\rm GRB}$, where $\rho_{\rm GRB}$ is the inferred occurrence rate of GRBs computed in Ref. [6]. Bearing the above in mind it is easy to check that there is a low probability for aLIGO to detect the GW signals associated with the GRB binary progenitors: indeed in the best case of the 2022+ observing rung one obtains, respectively, $\sim$ 1 detection every 3 and 5 yr for U-GRBs and S-GRFs.

References

[1] E.P. Mazets, S.V. Golenetskii, V.N. Ilinskii, V.N. Panov, R.L. Aptekar, I.A. Gurian, M.P. Proskura, I.A. Sokolov, Z.I. Sokolova, T.V. Kharitonova, Ap&SS**80**, 3 (1981)

[2] R.W. Klebesadel, *The durations of gamma-ray bursts*, in *Gamma-Ray Bursts - Observations, Analyses and Theories*, edited by C. Ho, R.I. Epstein, E.E. Fenimore (Cambridge University Press, 1992), pp. 161–168

[3] J.P. Dezalay, C. Barat, R. Talon, R. Syunyaev, O. Terekhov, A. Kuznetsov, *Short cosmic events - A subset of classical GRBs?*, in *American Institute of Physics Conference Series*, edited by W. S. Paciesas & G. J. Fishman (1992), Vol. 265 of *American Institute of Physics Conference Series*, pp. 304–309

[4] C. Kouveliotou, C.A. Meegan, G.J. Fishman, N.P. Bhat, M.S. Briggs, T.M. Koshut, W.S. Paciesas, G.N. Pendleton, ApJ**413**, L101 (1993)

[5] M. Tavani, ApJ**497**, L21 (1998), arXiv:astro-ph/9802192

[6] R. Ruffini, J.A. Rueda, M. Muccino, Y. Aimuratov, L.M. Becerra, C.L. Bianco, M. Kovacevic, R. Moradi, F.G. Oliveira, G.B. Pisani et al., ApJ**832**, 136 (2016), 1602.02732

[7] R. Ruffini, Y. Wang, M. Enderli, M. Muccino, M. Kovacevic, C.L. Bianco, A.V. Penacchioni, G.B. Pisani, J.A. Rueda, ApJ**798**, 10 (2015), 1405.5723

[8] R. Ruffini, M. Muccino, M. Kovacevic, F.G. Oliveira, J.A. Rueda, C.L. Bianco, M. Enderli, A.V. Penacchioni, G.B. Pisani, Y. Wang et al., ApJ**808**, 190 (2015), 1412.1018

[9] R. Ruffini, M.G. Bernardini, C.L. Bianco, L. Vitagliano, S.S. Xue, P. Chardonnet, F. Fraschetti, V. Gurzadyan, *Black Hole Physics and Astrophysics: The GRB-Supernova Connection and URCA-1 - URCA-2*, in *The Tenth Marcel Grossmann Meeting*, edited by M. Novello, S. Perez Bergliaffa, R. Ruffini (Singapore: World Scientific, 2006), p. 369, astro-ph/0503475

[10] L. Izzo, J.A. Rueda, R. Ruffini, A&A**548**, L5 (2012), 1206.2887

[11] J.A. Rueda, R. Ruffini, ApJ**758**, L7 (2012), 1206.1684

[12] C.L. Fryer, J.A. Rueda, R. Ruffini, ApJ**793**, L36 (2014), 1409.1473

[13] L. Becerra, F. Cipolletta, C.L. Fryer, J.A. Rueda, R. Ruffini, ApJ**812**, 100 (2015), 1505.07580

[14] C.L. Fryer, F.G. Oliveira, J.A. Rueda, R. Ruffini, Physical Review Letters **115**, 231102 (2015), 1505.02809

[15] L. Becerra, C.L. Bianco, C.L. Fryer, J.A. Rueda, R. Ruffini, ApJ**833**, 107 (2016), 1606.02523

[16] J. Goodman, ApJ**308**, L47 (1986)
[17] B. Paczynski, ApJ**308**, L43 (1986)
[18] D. Eichler, M. Livio, T. Piran, D.N. Schramm, Nature**340**, 126 (1989)
[19] R. Narayan, T. Piran, A. Shemi, ApJ**379**, L17 (1991)
[20] E. Berger, ARAA**52**, 43 (2014), 1311.2603
[21] F. Cipolletta, C. Cherubini, S. Filippi, J.A. Rueda, R. Ruffini, Phys. Rev. D**92**, 023007 (2015), 1506.05926
[22] C.L. Fryer, W. Benz, M. Herant, ApJ**460**, 801 (1996), astro-ph/9509144
[23] R.A. Chevalier, ApJ**346**, 847 (1989)
[24] Y.B. Zel'dovich, L.N. Ivanova, D.K. Nadezhin, Soviet Astronomy **16**, 209 (1972)
[25] R. Ruffini, J. Wilson, Physical Review Letters **31**, 1362 (1973)
[26] C.L. Fryer, F. Herwig, A. Hungerford, F.X. Timmes, ApJ**646**, L131 (2006), astro-ph/0606450
[27] C.L. Fryer, ApJ**699**, 409 (2009), 0711.0551
[28] L. Izzo, R. Ruffini, A.V. Penacchioni, C.L. Bianco, L. Caito, S.K. Chakrabarti, J.A. Rueda, A. Nandi, B. Patricelli, A&A**543**, A10 (2012)
[29] N.R. Tanvir, A.J. Levan, A.S. Fruchter, J. Hjorth, R.A. Hounsell, K. Wiersema, R.L. Tunnicliffe, Nature**500**, 547 (2013), 1306.4971
[30] N.R. Sibgatullin, R.A. Sunyaev, Astronomy Letters **26**, 772 (2000), astro-ph/0011344
[31] C.L. Fryer, S.E. Woosley, D.H. Hartmann, ApJ**526**, 152 (1999), astro-ph/9904122
[32] M. Dominik, K. Belczynski, C. Fryer, D.E. Holz, E. Berti, T. Bulik, I. Mandel, R. O'Shaughnessy, ApJ**759**, 52 (2012), 1202.4901
[33] K.A. Postnov, L.R. Yungelson, Living Reviews in Relativity **17**, 3 (2014), 1403.4754
[34] J.G. Hills, ApJ**267**, 322 (1983)
[35] LIGO Scientific Collaboration, J. Aasi, B.P. Abbott, R. Abbott, T. Abbott, M.R. Abernathy, K. Ackley, C. Adams, T. Adams, P. Addesso et al., Classical and Quantum Gravity **32**, 074001 (2015), 1411.4547
[36] V. Paschalidis, M. MacLeod, T.W. Baumgarte, S.L. Shapiro, Phys. Rev. D**80**, 024006 (2009)
[37] P.C. Peters, J. Mathews, Phys. Rev. **131**, 435 (1963)
[38] P.C. Peters, Phys. Rev. **136**, 1224 (1964)
[39] M. Rees, R. Ruffini, J.A. Wheeler, *Black holes, gravitational waves and cosmology* (Gordon and Breach Science Publishers Inc., New York, 1974)
[40] M. Davis, R. Ruffini, W.H. Press, R.H. Price, Phys. Rev. Lett. **27**, 1466 (1971)
[41] R. Ruffini, J. Rodriguez, M. Muccino, J.A. Rueda, Y. Aimuratov, U. Barres de Almeida, L. Becerra, C.L. Bianco, C. Cherubini, S. Filippi et al., ArXiv:1602.03545 (2016), 1602.03545
[42] É.É. Flanagan, S.A. Hughes, Phys. Rev. D**57**, 4535 (1998), gr-qc/9701039
[43] M. Rigault, G. Aldering, M. Kowalski, Y. Copin, P. Antilogus, C. Aragon, S. Bailey, C. Baltay, D. Baugh, S. Bongard et al., ApJ**802**, 20 (2015), 1412.6501
[44] B.P. Abbott, R. Abbott, T.D. Abbott, M.R. Abernathy, F. Acernese, K. Ackley, C. Adams, T. Adams, P. Addesso, R.X. Adhikari et al., Living Reviews in Relativity **19** (2016), 1304.0670
[45] L.S. Finn, D.F. Chernoff, Phys. Rev. D**47**, 2198 (1993)